GEOPHYSICAL RESEARCH LETTERS, VOL. 37, L10603, doi:10.1029/2010GL042827, 2010

Understanding the annual cycle of the Arctic Ocean bottom pressure

Cecilia Peralta-Ferriz[1] and James Morison[1]

Received 7 February 2010; revised 8 April 2010; accepted 21 April 2010; published 22 May 2010.

[1] Ocean bottom pressure (OBP) observations in the Arctic from *in situ* pressure recorders and the Gravity Recovery and Climate Experiment (GRACE) satellite mission, averaged over the basin, reveal annual oscillations of about 2 cm. The maximum occurs in late summer to early fall and the minimum in late winter to early spring. We derive a simple model of OBP response to runoff and precipitation minus evaporation (P-E) that agrees in phase with the observations and is 10% larger. **Citation:** Peralta-Ferriz, C., and J. Morison (2010), Understanding the annual cycle of the Arctic Ocean bottom pressure, *Geophys. Res. Lett.*, *37*, L10603, doi:10.1029/2010GL042827.

1. Introduction

[2] Seasonal variation is a dominant signal in Ocean Bottom Pressure (OBP) measured with *in situ* pressure gauges in the Arctic Ocean. The seasonal variations of the Arctic OBP have appeared in early releases of OBP measurements by the Gravity Recovery and Climate Experiment (GRACE) [*Ponte et al.*, 2007; *Morison et al.*, 2007] since 2002, and in numerical simulations [*Dobslaw and Thomas*, 2007].

[3] According to *Ponte et al.* [2007] GRACE release 2 from the Jet Propulsion Laboratory, and GRACE release 3 from Geo Forschungs Zentrum Potsdam, reveal a global average 1-cm water equivalent annual cycle in OBP with a maximum in the summer. Their GRACE results for the Arctic suggest a larger amplitude (2–3 cm) and a later peak (October). They suggest that the seasonal variation of the world ocean average OBP is the result of seasonality in Northern Hemisphere runoff and world ocean average atmospheric pressure.

[4] *Dobslaw and Thomas* [2007] show that the seasonal cycle in the Arctic OBP, averaging 1 cm peak to peak over the basin, is due to the seasonal cycle of runoff. Their modeled basin-averaged OBP is a little less than half the magnitude of the mass variation observed by GRACE, and the maximum simulated OBP is in July, earlier than the main peak observed by GRACE [*Ponte et al.*, 2007]. In addition, the simulations indicate that the seasonal OBP change is mainly barotropic, in agreement with general modeling results [*Vinogradova et al.*, 2007; *Gill and Niiler*, 1973].

[5] Runoff is the dominant meteoric water input to the Arctic Ocean (61%), followed by net precipitation minus evaporation (P-E, 39%), both with significant seasonal variations [*Serreze et al.*, 2006]. The ocean inflows to and outflows from the Arctic Ocean show seasonal fluctuation [e.g., *Woodgate and Aagaard*, 2005; *Schauer et al.*, 2004], but models without runoff driven only by wind do not show the seasonal mass change [*Dobslaw and Thomas*, 2007; *Zhang and Rothrock*, 2003]. This is likely because any pressure buildup in the Arctic Ocean due to ocean inflow acts to reduce the inflow or create a compensating outflow. In contrast, runoff and P-E are independent of ocean pressure. We might expect the addition of runoff mass to the Arctic Ocean to quickly propagate away to the rest of the world ocean at the barotropic wave speed. The model results by *Dobslaw and Thomas* [2007] show that runoff is retained in the Arctic Basin at seasonal time-scales, long enough to achieve a geostrophically balanced circulation. The observations indicate a lag in the OBP disturbance of about 2 months relative to the *Dobslaw and Thomas* [2007] model result.

[6] Here we provide a simple explanation for the observed annual cycle of the Arctic OBP by exploring Arctic Ocean GRACE and *in situ* OBP data, and deriving a simple physical model for the ocean response to runoff, P-E and atmospheric pressure.

2. Data

[7] We use GRACE monthly fields from the University of Texas Center for Space Research release 4 (CSR4), from August 2002 to May 2008 (http://grace.jpl.nasa.gov/data/mass/). The post-processing of the GRACE (CSR4) to obtain the time varying OBP from spherical harmonic gravity coefficients is explained by *Chambers* [2006a, 2006b]. The values represent anomalies relative to the mean from January 2003 to December 2006. We use data filtered [*Chambers*, 2006a, 2006b] with a Gaussian smoother with a 300 km half-amplitude radius. GRACE Arctic OBP is validated with measurements from two Arctic Bottom Pressure Recorders (ABPR) near the North Pole (89° 15.26′N, 60° 21.58′E and 89° 14.85′N, 148° 7.54′E), that report pressure every 15 minutes from April 2005 to April 2008. The data from the two ABPRs are well correlated with each other and agree well with GRACE [*Morison et al.*, 2007]. We also average well correlated OBP time series from three bottom pressure recorders (BPR) deployed annually by the Beaufort Gyre Exploration Project at a) 75° 0.449′N, 149° 58.660′W, b) 78° 1.49′N, 149° 49.203′W, and c) 76° 59.232′N, 139° 54.563′W, [http://www.whoi.edu/beaufortgyre/data_moorings.html] from August 2003 to August 2007. OBP data from Pressure Inverted Echo Sounders, September 2003 to August 2006 (A. Beszczynska-Möller, personal communication, 2007), were averaged to give a time-series of OBP in Fram Strait. The *in situ* pressure records were de-tided using the

[1]Polar Science Center, Applied Physics Laboratory, University of Washington, Seattle, Washington, USA.

0094-8276/10/2010GL042827

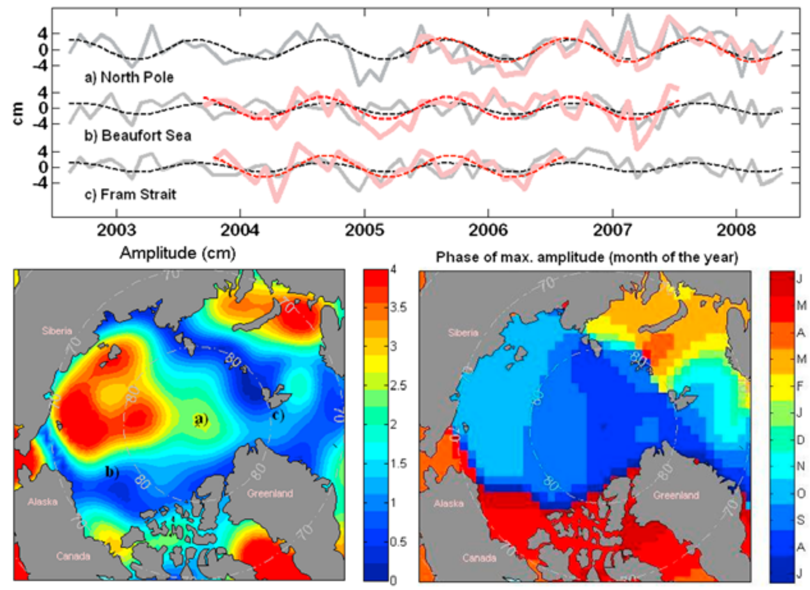

Figure 1. (top) Time-series of monthly averages of *in situ* (shaded red) OBP anomaly, and their respective annual harmonic fit (dashed red) at the North Pole, Beaufort Sea and Fram Strait (letter coded in the map on the bottom left). GRACE OBP at each location is shown in grey, and the annual cycle in dashed black lines. All the time-series have a long term linear trend removed. (bottom left) Amplitude and (bottom right) phase of the GRACE OBP annual fit.

T_TIDE MATLAB analysis program of *Pawlowicz et al.* [2002], and averaged to the same 30-day bins as GRACE.

[8] We use monthly averages of atmospheric sea level pressure (SLP) from the NCEP/NCAR reanalysis [*Kalnay et al.*, 1996] (http://dss.ucar.edu/pub/reanalysis/). Like GRACE, the SLP anomalies are estimated relative to the average from Jan. 2003 to Dec. 2006.

[9] We use runoff data from the Arctic-Regional, Integrated Hydrological monitoring System (Arctic-RIMS) provided by the Water Systems Analysis Group (http://rims.unh.edu/) and from the Regional, Electronic and Hydrographic Data Network for the Arctic Region (R-Arctic Net, http://www.r-arcticnet.sr.unh.edu/v3.0/). Total runoff is dominated by the gauged runoff of the major rivers: Yenisey, Ob, Pechora, Kolyma, Lena, Severnaya Dvina and Mackenzie. Smaller gauged rivers add 12% to this amount. *Dobslaw and Thomas* [2007] assumed that ungauged runoff accounted for 22% of the total. We assume that the ungauged part amounts 30% of the total runoff [*World Climate Research Program*, 1998], in agreement with hydrologic model results [*Su et al.*, 2005]. Consequently, we take total runoff as 1.6 times the contribution of the 7 major rivers. We use climatology data of precipitation minus evaporation (P-E) from ERA-40 [*Serreze et al.*, 2006].

3. Seasonal Cycle

[10] GRACE and *in situ* OBP measurements from the North Pole, Beaufort Gyre and Fram Strait show good agreement and a common seasonal signal (Figure 1, top), indicative of variation in the Arctic OBP at basin-wide scale in Central Arctic. The fit of an annual harmonic to the GRACE OBP time-series of the Arctic Ocean (Figure 1, bottom) shows the maximum OBP occurring in August–October in the Central Arctic. The maximum OBP in the Barents and Kara Seas is in early spring. The amplitude of the basin-averaged GRACE OBP annual cycle is 2 cm peak to peak, about twice the amplitude of the *Dobslaw and Thomas* [2007] model, but consistent with *Ponte et al.* [2007], with the phase of maximum amplitude in September. The annual harmonic fit to the basin-averaged OBP explains 15% of the variance of the OBP signal. This indicates the OBP is highly variable at shorter than seasonal time scales. In more localized regions, the amount of variance explained by an annual fit to the GRACE observations of OBP reaches about 50% in the East Siberian Sea, 60% in the Barents Sea and 25% at the North Pole.

4. Simple Model of Seasonal OBP Variation

[11] Possibly the simplest model of the Arctic Ocean is a rotating tank with a narrow channel connecting it to the world ocean. As meteoric water pours into the middle of the tank in a seasonal cycle, the changes in sea surface height and hydrostatic pressure are geostrophically balanced, producing anticyclonic flow through most of the water column. There is an ageostrophic radial flow only in the bottom boundary layer where the flow turns down pressure gradient. For most of the tank where there is no channel, there is a helical secondary flow outward at the bottom and inward at the surface, but at the channel opening, ocean mass is able to leak out radially in the bottom boundary layer, decreasing water volume in the tank.

[12] For a meteoric input (runoff + P-E) with a mean annual component and seasonal variation, the annual mean input would result in a surface displacement in the tank sufficient to drive equivalent leakage through the bottom boundary layer in the channel. The degree to which ocean mass can build up seasonally depends on the degree of leakage in the bottom boundary layer, which in turn depends on the bottom stress at the mouth of the channel. If the leakage path were unrestricted, the seasonal buildup in

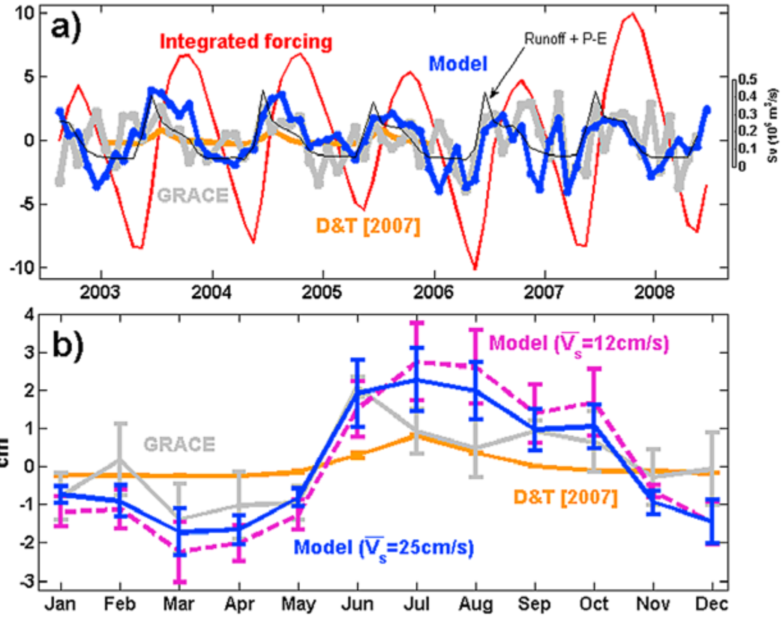

Figure 2. (a) GRACE OBP averaged over the Arctic (gray); monthly basin-averaged OBP derived from the model (blue); time-integral of the forcing over the basin minus a linear trend (red); the basin-averaged modeled OBP from *Dobslaw and Thomas* [2007] (orange); and forcing of the model (runoff + P-E) as thin black line along with its own scale on the right. (b) Monthly means (centered in day 15) of OBP from GRACE (gray), our model with enhanced mixing (blue), model without enhanced mixing (dashed magenta) and *Dobslaw and Thomas* [2007] (orange). Vertical bars are the standard error of the modeled and observed OBP.

ocean mass would be small and in phase with the input. Actually, the Arctic Ocean seasonal OBP variation is nearly in phase with and half the amplitude of the time-integral of the seasonal variation in meteoric forcing (Figure 2a). This suggests that the leakage of meteoric input from the Arctic Ocean is restricted but not completely.

[13] The conceptual model for temporal change in Arctic Ocean mass can be expressed as

$$A\frac{dh}{dt} = F(t) - \frac{L}{\rho f}\tau_b^x(t) \qquad (1)$$

where A is the area of the Arctic Ocean (9×10^{12} m^2); h is the ocean surface displacement and F is the volume input (runoff plus P-E); t is time. The second term on the right represents the leakage, given by the Ekman transport in the bottom boundary layer, where τ_b^x is the bottom shear stress in the zonal direction [*Gill*, 1982]. L is the width of the channel where the flow exits the basin, ρ is the average density of the sea water (1025 kg/m^3), f is the Coriolis parameter. Bottom stress can be expressed in terms of the geostrophic velocity away from the boundary [*Gill*, 1982]:

$$\tau_b^x(t) = \rho C_d V_s^2 \cos(\alpha) \qquad (2)$$

Here, C_d is the bottom drag coefficient, and α is the turning angle of the flow within the bottom boundary layer.

[14] In the model, the resulting ocean mass change h can be thought of as sea surface height (SSH) change in this barotropic model. OBP variations are the sum of the SLP changes and the variations of the ocean mass. Therefore, the basin-averaged SLP added to the ocean response h from the model gives the modeled OBP. $V_s = (g/f)(\Delta h/\Delta y)$ is the scaled geostrophic velocity in terms of the pressure difference ($\Delta h = h + P_a - P_{bo}$) inside and outside the basin over a distance Δy, where P_a is the basin-averaged SLP variation and P_{bo} is the averaged OBP variation outside, given by the global ocean mean of OBP [*Ponte et al.*, 2007]. L, taken as 2×10^6 m, represents the approximate width of the exit path from the Arctic Ocean at Fram Strait, across the Barents Sea shelf edge to the Norwegian Sea, and a contribution for the Canadian Archipelago. We take $\Delta y = 0.25 \times 10^6$ m as a representative distance through Fram Strait and across the gateway to the Barents Sea.

[15] Assuming that no other physics at the bottom boundary occur besides the seasonal response to meteoric water and SLP, and using reasonable values of C_d, the amplitude of the modeled OBP is in phase with but larger than the observed. This suggests that insufficient leakage is occurring in the bottom boundary layer, likely because the background non-seasonal velocity associated with the mean wind driven circulation and other factors is ignored. This background velocity is much larger than the seasonal variation due to runoff, so ignoring it results in erroneously low levels of bottom boundary layer turbulence. Enhanced turbulence thickens the boundary layer and increases the seasonally varying Ekman transport at the bottom. In order to account for the effect of steady background currents, we assume the velocity is the sum of the seasonally varying part and a mean part, $\overline{V}_s$, dominated by an ambient background velocity, V_{amb}, and linearize equation (1):

$$A\frac{dh}{dt} = F(t) - \frac{LC_d}{f}\overline{V}_s^2\cos(\alpha) - \frac{2LC_d}{f}\cos(\alpha)\overline{V}_s\frac{g}{f}\frac{[h'(t) + P_a'(t) - P_{bo}'(t)]}{\Delta y} \qquad (3)$$

where $\overline{V}_s = V_{amb} + (g/f)([\overline{h} + \overline{P}_a - \overline{P}_{bo}]/\Delta y)$. Bars indicate the time-independent average and primes indicate pertur-

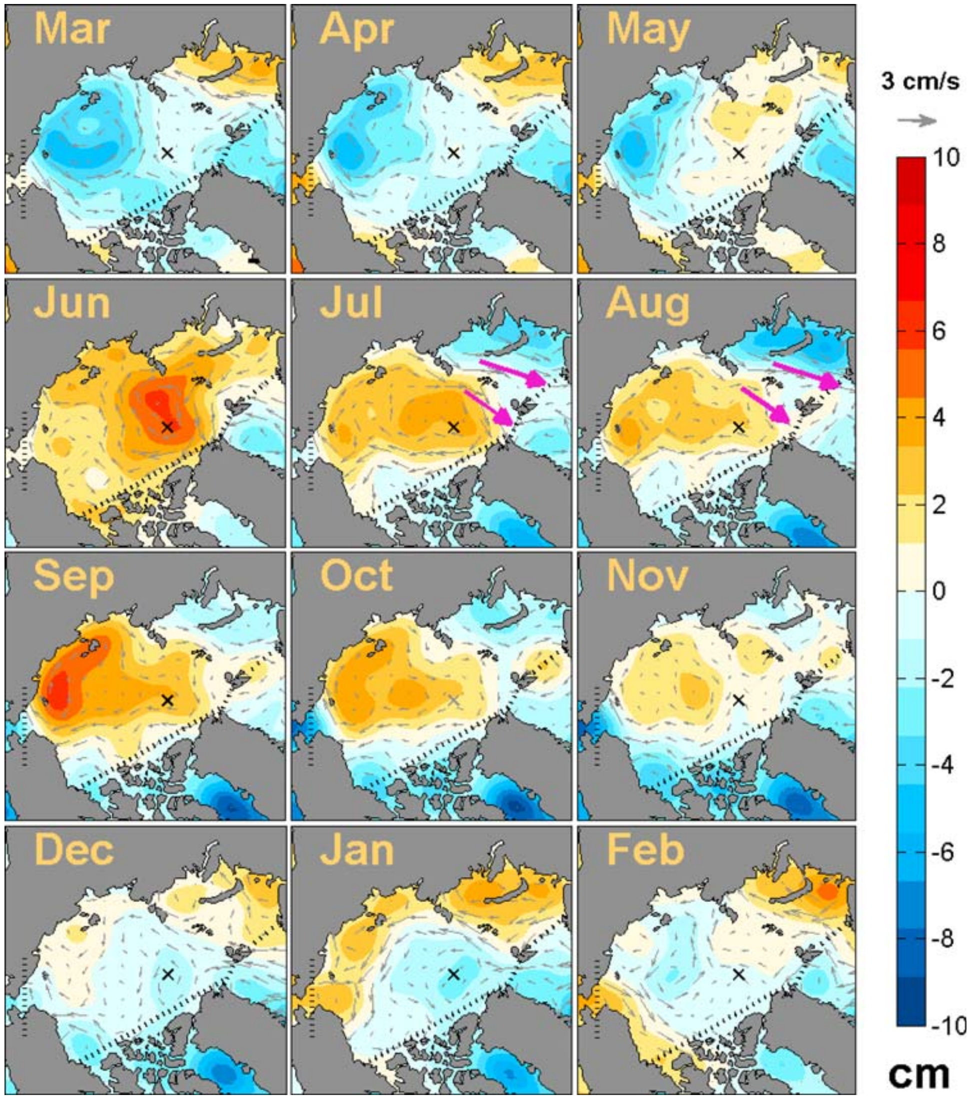

Figure 3. Color contours show the monthly means of GRACE OBP; the gray arrows show the geostrophic velocity due to OBP gradient; black dotted lines show the boundary of the area that accounts for the basin-averaged OBP. The magenta arrows emphasize the geostrophic-leak out of the basin.

bation. The right hand side of equation (3) includes time-independent and time-varying terms. The perturbation part of equation (3) (last term of the right hand side) gives the seasonally varying response. Background velocity estimates in the Fram Strait, Barents shelf-break gateway region range from 5 cm/s [*Schauer et al.*, 2004] to 25 cm/s [*Hanzlick*, 1983; F. Nilsen, personal communication, 2009]. For this study, we start by assuming a background velocity of 12 cm/s, much larger than the runoff–induced seasonal variation.

[16] We estimate a value for C_d and α using the Rossby similarity drag law [*McPhee*, 2008] applied to the benthic boundary layer. With this universal relation and assuming stable and near neutral stratification, the relation of surface stress to velocity outside the boundary layer is dependent on the boundary layer surface roughness scale, z_o. For the abyssal benthic layer (i.e., generally flat, relatively smooth surface), z_o is ~1 cm (M. McPhee, personal communication, 2009); for much rougher underside of sea-ice, $z_o \sim 3$ cm is typical [*McPhee*, 2008]. We would expect the roughness length scale in the Fram Strait–Barents shelf-break region to lie between these values. Here we use $z_o = 2$ cm. According to the Rossby similarity, C_d is weakly dependant on velocity. For 12 cm/s and $z_o = 2$ cm, C_d is 4.3×10^{-3} and α is 18.8°.

5. Model Results

[17] We spin up the model for 10 years using repeated monthly means of the meteoric forcing from 2002–2008. A steady state is reached within one year, with a mean SSH increase of ~0.35 m (i.e., $\Delta\overline{h}$). After a year, the time-varying response is dominated by the seasonal variations. With $\overline{V}_s$ = 12 cm/s, the simulated seasonal variation of amplitude ~2.3 cm is in general agreement in phase and slightly larger than the monthly values of the basin-averaged observed OBP (Figure 2b). The amplitude of the modeled OBP variations is reduced by a factor of about 2 relative to the simple time-integral of the seasonal meteoric input. As with *Dobslaw and Thomas* [2007], our model response is dominated by runoff,

with a smaller contribution of P-E. The maximum model response without atmospheric pressure forcing, P_a, is slightly larger (~8%) than with P_a, and advanced in phase by a couple of months relative to the phase of the observed OBP.

[18] The RMS-difference between GRACE and our modeled OBP is ~1.2 cm (Figure 2b), with the maximum differences in the months of July and August. The RMS difference is in part due to OBP variations at shorter than seasonal time scales (e.g., 19 days [*Morison*, 1991]) that are not related to the runoff and pressure forcing used in the model.

[19] The RMS-difference associated with seasonal cycle can be partly reduced by additional enhancement of mixing to increase the leakage. We illustrate this by assuming a larger value of $\overline{V}_s$, 25 cm/s ($C_d = 3.7 \times 10^{-3}$ and $\alpha = 17.5°$). One rationale for such an enhancement is that it would represent mixing produced by the higher frequency or smaller scale processes such as tides, eddies, internal waves and winter time convection on the shelves [e.g., *Saloranta and Svendsen*, 2001; *Teigen et al.*, 2010]. The enhancement reduces the RMS difference from observed OBP to 0.85 cm (Figure 2b).

[20] However, as shown by comparison of the monthly mean values, even with enhanced mixing, the model response is consistently higher than the observed OBP in July and August (Figure 2b). The observed OBP drops slightly after the increase in June that coincides with the peak in annual runoff. We do not think this is due to semi-annual or 161-day (K2 tidal alias) errors in GRACE because harmonic fits at these periods to the observed OBP (semi-annual ~ 0.3 cm and 161-day ~ 0.05 cm) are much smaller and explain less variance (1.7% and 0.04%) than the annual fit (amplitude ~1 cm, 15% of variance). We think the difference is likely due to leakage during July and August that represents departure of the Arctic Ocean from the one-dimensional rotating tank analogy. This is illustrated by spatial distribution of the monthly means of observed OBP (Figure 3). May shows a positive OBP anomaly spreading from the Kara Sea, a region of numerous large rivers, out toward the North Pole. This develops in June to the largest positive monthly OBP anomaly as a basin-wide closed cell of anticyclonic circulation analogous to our idealized model. During July and August the closed nature of the cell breaks down and appears to interact with the Fram Strait-Barents Sea geography to possibly direct at least a fraction of the geostrophic flow out of the Arctic Ocean. The break down of the cell may occur because ageostrophic leakage first increases mass in the Barents Sea. Alternatively, Ekman pumping due to summer time northeasterly winds may shift ocean mass to form the OBP dipole between the Central Arctic (high pressure) and the Barents Sea (low pressure). Diversion of a small fraction of the total geostrophic flow due to the dipole could eliminate the July–August model-observed OBP difference, accounting for 30% of the RMS difference between the model and observed OBP. In September and October, the flow appears more nearly closed by a center of high OBP that develops at the exit path.

6. Conclusion

[21] The idealized rotating tank model driven by runoff, and to a lesser degree by seasonal variation of P-E and atmospheric pressure, shows reasonable agreement with observed seasonal variation in Arctic Ocean average bottom pressure. To achieve the best agreement, it is necessary to maximize leakage by non-geostrophic Ekman transport in the bottom boundary layer of the exit channel by enhancing turbulence and hence bottom stress for a given OBP anomaly. We believe the enhanced turbulence is largely explained and well parameterized by a background current, larger than the seasonally varying current, which represents observed mean currents in the exit regions. Additional enhancement is also justified for short time-scale processes that increase turbulence. The model OBP response to runoff alone peaks in early to mid summer near the time of peak runoff, but tails off more slowly than runoff. The added effect of average atmospheric pressure variation helps to reduce the model peak response and shift the peak toward the end of summer in agreement with observations. The analogy between the Arctic Ocean and the idealized model appears to break down in July–August as the observed OBP drops toward Fram Strait and the anticyclonic OBP cell spreads toward Svalbard to possibly vector a portion of geostrophic flow out of the Basin. This geostrophic flux would reduce actual OBP relative to the idealized model with only ageostrophic bottom boundary layer leakage.

[22] **Acknowledgments.** We thank John Wahr and Ron Kwok for their help and anonymous reviewers for their helpful comments. This work was supported by NSF grant OPP-0326109 and NASA grant NNX08AH62G.

References

Chambers, D. P. (2006a), Observing seasonal steric sea level variations with GRACE and satellite altimetry, *J. Geophys. Res.*, *111*, C03010, doi:10.1029/2005JC002914.

Chambers, D. P. (2006b), Evaluation of new GRACE time-variable gravity data over the ocean, *Geophys. Res. Lett.*, *33*, L17603, doi:10.1029/2006GL027296.

Dobslaw, H., and M. Thomas (2007), Impact of river run-off on global ocean mass redistribution, *Geophys. J. Int.*, *168*(2), 527–532, doi:10.1111.j.1365-246X.2006.03247.x.

Gill, A. E. (1982), *Atmosphere-Ocean Dynamics*, 662 pp., Academic, New York.

Gill, A. E., and P. Niiler (1973), The theory of seasonal variability in the ocean, *Deep Sea Res.*, *20*, 141–177.

Hanzlick, D. J. (1983), The West Spitsbergen Current: Transport, forcing and variability, Ph.D. dissertation, 127 pp., Uni. of Wash., Seattle.

Kalnay, E., et al. (1996), The NCEP/NCAR 40-year reanalysis project, *Bull. Am. Meteorol. Soc.*, *77*, 437–471, doi:10.1175/1520-0477(1996)077<0437:TNYRP>2.0.CO;2.

McPhee, M. (2008), *Air-Ice-Ocean Interaction: Turbulent Ocean Boundary Layer Exchange Processes*, 215 pp., Springer, New York.

Morison, J. (1991), Seasonal variations in the West Spitsbergen Current estimated from bottom pressure measurements, *J. Geophys. Res.*, *96*(C10), 18,381–18,395, doi:10.1029/91JC01916.

Morison, J., J. Wahr, R. Kwok, and C. Peralta-Ferriz (2007), Recent trends in Arctic Ocean mass distribution revealed by GRACE, *Geophys. Res. Lett.*, *34*, L07602, doi:10.1029/2006GL029016.

Pawlowicz, R., B. Beardsley, and S. Lentz (2002), Classical tidal harmonic analysis including error estimates in MATLAB using T_TIDE, *Comput. Geosci.*, *28*, 929–937, doi:10.1016/S0098-3004(02)00013-4.

Ponte, R. M., K. J. Quinn, C. Wunsch, and P. Heimbach (2007), A comparison of model and GRACE estimates of the large-scale seasonal cycle in ocean bottom pressure, *Geophys. Res. Lett.*, *34*, L09603, doi:10.1029/2007GL029599.

Saloranta, T. M., and H. Svendsen (2001), Across the Arctic front west of Spitsbergen: High resolution CTD sections from 1998–2000, *Polar Res.*, *20*(2), 177–184, doi:10.1111/j.1751-8369.2001.tb00054.x.

Schauer, U., E. Fahrbach, S. Osterhus, and G. Rohardt (2004), Arctic warming through the Fram Strait: Oceanic heat transport from 3 years of measurements, *J. Geophys. Res.*, *109*, C06026, doi:10.1029/2003JC001823.

Serreze, M. C., A. P. Barrett, A. G. Slater, R. A. Woodgate, K. Aagaard, R. B. Lammers, M. Steele, R. Moritz, M. Meredith, and C. M. Lee

(2006), The large-scale freshwater cycle of the Arctic, *J. Geophys. Res.*, *111*, C11010, doi:10.1029/2005JC003424.
Su, F., J. C. Adam, L. C. Bowling, and D. P. Lettenmaier (2005), Streamflow simulations of the terrestrial Arctic domain, *J. Geophys. Res.*, *110*, D08112, doi:10.1029/2004JD005518.
Teigen, S. H., F. Nilsen, and B. Gjevik (2010), Barotropic instability in the West Spitsbergen Current, *J. Geophys. Res.*, doi:10.1029/2009JC005996, in press.
Vinogradova, N., R. M. Ponte, and D. Stammer (2007), Relation between sea level and bottom pressure and the vertical dependence of oceanic variability, *Geophys. Res. Lett.*, *34*, L03608, doi:10.1029/2006GL028588.
Woodgate, R. A., and K. Aagaard (2005), Revising the Bering Strait freshwater flux into the Arctic Ocean, *Geophys. Res. Lett.*, *32*, L02602, doi:10.1029/2004GL021747.
World Climate Research Program (1998), Report of the ACSYS workshop on status and directions for the Arctic runoff data base. Arctic climate system study, report, Geneva Switzerland.
Zhang, J., and D. A. Rothrock (2003), Modeling global sea ice with a thickness and enthalpy distribution model in generalized curvilinear coordinates, *Mon. Weather Rev.*, *131*, 845–861.

J. Morison and C. Peralta-Ferriz, Polar Science Center, Applied Physics Laboratory, University of Washington, 1013 NE 40th St., Seattle, WA 98105, USA. (morison@apl.washington.edu; ferriz@u.washington.edu)